View Article Online
View Journal

Dalton Transactions

An international journal of inorganic chemistry

Accepted Manuscript

This article can be cited before page numbers have been issued, to do this please use: B. Kripli, M. I. Szávuly, F. V. Csendes and J. Kaizer, *Dalton Trans.*, 2020, DOI: 10.1039/C9DT04551A.

ROYAL SOCIETY OF CHEMISTRY

rsc.li/dalton

View Article Online
DOI: 10.1039/C9DT04551A

Journal Name

COMMUNICATION

Functional models of nonheme diiron enzymes: reactivity of μ-oxo-μ-1,2-peroxo-diiron(III) intermediate in electrophilic and nucleophilic reactions.

Received 00th January 20xx,
Accepted 00th January 20xx

DOI: 10.1039/x0xx00000x

www.rsc.org/

Balázs Kripli, Miklós Szávuly, Flóra Viktória Csendes, and József Kaizer*

Dedicated to Professor Gábor Speier on the occasion of his 80th birthday.

Abstract: The reactivity of the previously reported peroxo-adduct $[Fe^{III}_2(\mu\text{-}O)(\mu\text{-}1,2\text{-}O_2)(IndH)_2(solv)_2]^{2+}$ (1) (IndH = 1,3-bis(2-pyridyl-imino)isoindoline) has been investigated in nucleophilic (e.g., deformylation of alkyl and aryl alkyl aldehydes) and electrophilic (e.g. oxidation of phenols) stoichiometric reactions as biomimics of ribonucleotide reductase (RNR-R2) and aldehyde deformylating oxygenase (ADO) enzymes. Based on detailed kinetic and mechanistic studies we have found further evidence for the ambiphilic behaviour of the peroxo intermediates proposed for diferric oxidoreductase enzymes.

Nonheme dinuclear oxidoreductases such as ribonucleotide reductase (RNR),[1] arylamine *N*-oxygenase (CmII),[2] deoxyhypusine hydroxylase (hDOHH),[3] soluble methane monooxygenase (sMMO),[4] and toluene monooxygenase (TMO)[5] generate high-valent $Fe^{III}Fe^{IV}$ (RNR-R2) or $Fe^{IV}Fe^{IV}$ (CmII, hDOHH, sMMO and TMO) oxoiron species via peroxo-diiron(III) intermediates as a result of dioxygen activation.[6] These intermediates are responsible for many types of electrophilic and nucleophilic oxidative process in the aforementioned enzymes and their synthetic models. For example, the sMMO and RNR enzymes catalyse the oxidation of alkanes and phenols via electrophilic C-H and O-H activation, respectively, whilst the aldehyde deformylating oxygenases (ADO)[7] catalyse the aldehyde deformylation with a nucleophilic mechanism. The ambiphilic feature of these enzymes can be interpreted with the involvement of two distinct oxidants, namely the electrophilic high-valent oxoiron(IV) and the nucleophilic peroxo-diferric intermediates. While, the reactivity of oxoiron(IV) species in various electrophilic reactions have been studied in details, only few examples can be seen in the literature, where peroxo-metal species are the key reactive intermediates. Furthermore, understanding the factors that lead to O–O bond cleavage at nonheme diiron centers resulting electrophilic intermediate has also been a major goal of researchers in this field, to get more insight into the versatility of this family of enzymes. It can be found some biologically relevant mononuclear end-on copper(II)-,[8] and iron(III)-superoxides,[9] and dinuclear diiron(II,III)-superoxide that was capable of electrophilic hydrogen atom abstraction (HAA) from phenols,[10] intramolecular C-H activation and oxygen atom transfer reactions (OAT), but only few examples can be found in the literature, where peroxo-metal complexes are directly involved in a nucleophilic reaction (e.g., the deformylation of aldehydes).[11] McDonald and Que had previously reported the first example of a reactive dimanganese(II,III)-peroxide as nucleophilic oxidant.[12]

To date, around 30 synthetic spectroscopically characterized peroxo-diferric complexes are known as possible stuctural models of diiron enzymes.[13] As a possible functional model of RNR-R2 and ADO enzymes we have investigated the reactivity of peroxo adduct $[Fe_2(\mu\text{-}O_2)(MeBzim\text{-}Py)4(CH_3CN)]^{4+}$ (**2**, MeBzim-Py = 2-(2'-pyridyl)-*N*-methylbenzimidazole) towards various phenols and aldehydes.[13a,b] In the former case we have found direct kinetic and computational evidence for the formation of low-spin oxoiron(IV) species and its involvement as an electrophilic species in the O-H activation process,[13a] whilst in the latter case the μ-1,2-peroxo-diiron(III) intermediate proved to be a nucleophilic oxidant in the aldehyde deformylation, that occurs by Baeyer-Villiger type mechanism including rate-limiting A_N or Creege-type

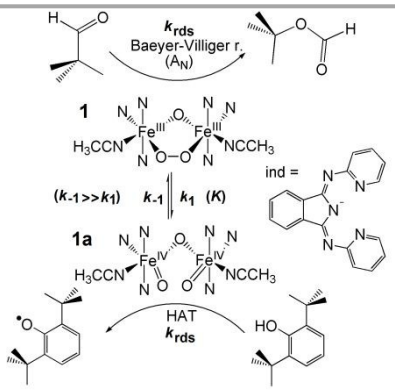

Scheme 1. Electrophilic (phenol oxidation) and nucleophilic (aldehyde deformylation) reactions of **1**.

Department of Chemistry, University of Pannonia, H-8201 Veszprém, Hungary
E-mail: kaizer@almos.uni-pannon.hu.†Electronic Supplementary Information (ESI) available: Experimental details of oxidations, and kinetic data. See DOI: 10.1039/x0xx00000x

rearrangement steps depending on the substrate used.[13b] As a continuity of this study we have choosed the previously reported and fully characterized (μ-oxo)-(μ-1,2-peroxo)-diiron(III) species, $[Fe^{III}_2(\mu\text{-}O)(\mu\text{-}1,2\text{-}O_2)(IndH)_2(solv)_2]^{2+}$ (**1**, IndH = 1,3-bis(2-pyridylimino)isoindoline) as model compound,[14] where the dissociation of the diiron(III) core may be excluded due to the μ-oxo-bridge, and investigated its reactivity compared to our earlier system ($[Fe_2(\mu\text{-}O_2)(MeBzim\text{-}Py)_4(CH_3CN)]^{4+}$)[13a,b] (**2**) in both electrophilic and nucleophilic reactions to get further evidence for the ambiphilic behaviour of a μ-1,2-peroxo-diiron intermediates proposed for diiron oxygenases.[6]

Initially we have investigated the electrophilic and nucleophilic reactivity of the in situ generated $[Fe^{III}_2(\mu\text{-}O)(\mu\text{-}1,2\text{-}O_2)(IndH)_2(solv)_2]^{2+}$ (**1**) (derived from the reaction of $[Fe^{II}(IndH)(solv)_3]^{2+}$ with stoichiometric amounts of H_2O_2) towards benzaldehyde (PhC(O)H) as electrophilic and 2,6-di-*tert*-butylphenol (DTBPH) which may behave either as nucleophilic or electrophilic model substrates in CH_3CN at 10 ˚C, and obtained the same results that benzoic acid[13b] and 3,3',5,5'-tetra-*tert*-butyl-4,4'-diphenoquinone[13a] were produced as major products (80-80 % based on **1**, Fig. S2 and S3, ESI), respectively. The distinction between nucleophilic versus radical peroxo character can be proved with phenols since deprotonation leads to phenoxide coordination, whereas HAA provides a phenoxyl radical, which can lead to an easily-identifiable 2,2'-biphenol-coupled product after the disproportionation of the forming semiquinones. Based on our previous kinetic and computational results peroxo O–O bond cleavage resulting in oxoiron(IV) intermediate (**1a**) may also occur prior to HAA in these reactions. Complex **1** decays over the course of 200 s at 10 °C with k_{decay} = 3.5(5) × 10^{-3} s^{-1} with a large $\Delta H^{‡}$ of 81(3) kJ mol^{-1} and a small $\Delta S^{‡}$ of -10(10) J mol^{-1} K^{-1} (Fig. S1), which is consistent with an unimolecular decay process. The decay rate of **1**, which was monitored by UV-vis spectroscopy at 690 nm (Fig. 1, ESI),[14] is significantly increased by the addition of PhC(O)H or DTBPH, and the extent of which is linearly dependent on the concentration of the substrate in both cases (Fig. 2A). These results indicate a direct reaction between **1** and PhC(O)H, and **1a** and DTBPH with k_2 = 2.16±0.08 M^{-1} s^{-1} and k_2 = 0.40±0.01 M^{-1} s^{-1}, respectively at 10 °C. The activation parameters for PhC(O)H and DTBPH are $\Delta H^{‡}$ = 28(1) kJ mol^{-1}, $\Delta S^{‡}$ = -138(3) J mol^{-1} K^{-1}, $\Delta G^{‡}$ = 69(2) kJ mol^{-1}, and $\Delta H^{‡}$ = 27(4) kJ mol^{-1}, $\Delta S^{‡}$ = -175(14) J mol^{-1} K^{-1}, $\Delta G^{‡}$ = 79(8) kJ mol^{-1} at 10 °C, respectively (Fig. 2B). The activation enthalpy of 28 kJ mol^{-1} and the calculated Gibbs energy of 69 kJ mol^{-1} for PhC(O)H are smaller than those observed for **2**/PhC(O)H system ($\Delta H^{‡}$ = 42 and $\Delta G^{‡}$ = 71 kJ mol^{-1}), which is consistent with the higher reactivity of **1** with PhC(O)H.[13b] Similarly, under identical conditions the $\Delta H^{‡}$ = 27 kJ mol^{-1} and $\Delta G^{‡}$ = 79 kJ mol^{-1} values are smaller than that was obtained for **2**/DTBPH (64 and 96 kJ mol^{-1}),[13a] but larger than that calculated for $[Fe^{IV}(N4Py^*)(O)]^{2+}$/DTBPH ($\Delta H^{‡}$ = 21 and $\Delta G^{‡}$ = 42 kJ mol^{-1}, N4Py* = *N*,*N*-bis(2-pyridylmethyl)-1,2-di(2-pyridyl)-ethylamine).[15] Compared to the self-decay process, the much smaller $\Delta H^{‡}$ and the large, negative $\Delta S^{‡}$ values are consistent with an associative-type bimolecular reactions. A k_{rel}(PhC(O)H/DTBPH) value of 5.4 was also determined by comparing the individual reactions under identical conditions. The kinetics of benzaldehyde and phenol oxidation have also been measured with PhC(O)D and DTBPD to investigate the C-H and O-H kinetic isotope effects (*KIE*). In the former case the almost identical rate constant when compared with PhC(O)H suggests that the benzylic (aldehydic) hydrogen atom is innocent, its involvement in the rate-determining step can be excluded. In the latter case the involvement of the phenolic O-H bond in the rate-determining step is indicated by the magnitude of the $k_{O\text{-}H}/k_{O\text{-}D}$ *KIE* (*SIE*) of 1.8 in CH_3CN/H_2O and CH_3CN/D_2O. The observed isotope effect is not large, but SIE in HAA reactions are not necessarily large due to the involvement of proton transfer and/or disruption of hydrogen bonding in the presence of water. This value is almost identical with the data reported for the previously published **2**/DTBPH system (*KIE* = 1.78),[13a] and comparable to those obtained with mononuclear complexes $[Fe^{IV}(N4Py^*)(O)]^{2+}$ (*KIE* = 4.5 for DTBPH),[15] and $[Fe^{IV}(TMC)(O)(X)]^{2+}$ (*KIE* = 2.7 for H_2Q[16] (H_2Q = 1,4-hydroquinone, TMC = 1,4,8,11-tetramethyl-1,4,8,11-tetraaza-cyclotetradecane). These values are much smaller than those for corresponding oxidations, where the reactions

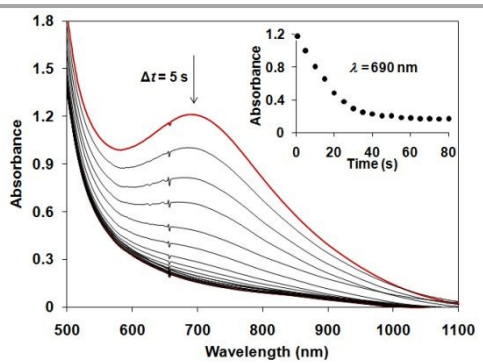

Fig. 1. Reactions of **1** with benzaldehyde in CH_3CN at 10 ˚C: UV-vis spectral change of **1** (1 mM) upon addition of 20 equiv. PhCHO. Inset shows time course of the decay of **1** monitored at 690 nm upon addition of 20 equiv. PhCHO.

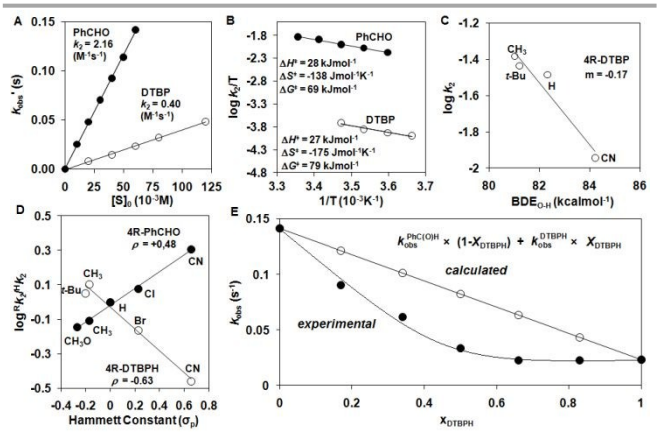

Fig. 2. Reactions of $[Fe^{III}_2(\mu\text{-}O)(\mu\text{-}1,2\text{-}O_2)(IndH)_2(solv)_2]^{2+}$ (**1**) with 4R-PhC(O)H and 4R-DTBPH (R = CH_3O, CH_3, H, Cl, CN and *t*-Bu, CH_3, H, Br, CN) in CH_3CN at 10 °C. (A) Plot of k_{obs}' versus [substrate] for reactions of **1** (1 mM) with PhCHO, and DTBPH. (B) Eyring plots of logk_2/T versus 1/T for PhC(O)H and DTBPH. (C) Plot of logk_2 versus $BDE_{O\text{-}H}$ for DTBPH. (D) Hammett plots of log k_{rel} against σ_p of 4R-PhC(O)H and 4R-DTBPH. (E) Competitive oxidation of PhC(O)H and DTBPH: [**1**] = 1 mM; [PhC(O)H + DTBPH] = 60 mM.

occur by proton-coupled electron transfer (PCET) mechanism (e.g., *KIE* = 29 for *cis*-$[Ru^{IV}(bpy)_2(py)(O)]^{2+}$/$H_2Q$).[17a] Consistent with a HAA mechanism, studies with *para*-substituted 2,6-di-*tert*-butylphenols (4R-DTBPH, R = *t*-Bu, CH_3, H, Br, CN) afforded a linear correlation between the reaction rates and the O-H bond dissociaton energy (BDE_{O-H}) values of the substrates. The slope of -0.17 is little bit smaller (Fig. 2C), but comparable to those obtained in the oxidation of 4R-DTBPHs by $[Fe^{IV}(N4Py^*)(O)]^{2+}$ (-0.48),[16] and $[Fe^{IV}(TMC)(O)(X)]^{2+}$ (X = N_3 (-0.36), CF_3CO_2 (-0.42) and CH_3CN (-0.55)) via HAA mechanism.[17b] Further evidence for a HAA derives from the Hammett analysis of the rate data from the DTBPH derivatives. Plotting the relative rates ($\log({}^{R}k_2/{}^{H}k_2)$) as a function of σ_p and σ_p^+ values of the substituents afford ρ value of -0.63 and -0.58, which is almost identical with the data observed for **2**/DTBPH (-0.71),[13a] and suggests that the metal-based oxidant is electrophilic (Fig. 2D). Furthermore, these relatively small negative values suggest that there is a small development of positive charge on the substrate in the transition state, and that the phenol oxidation in our case occurs by H atom abstraction, excluding the electron transfer process, which typically shows a more negative ρ value due to the more polar transition state.

To probe the nucleophilic reactivity of **1** we have investigated the electronic effect of substrates with para-substituted benzaldehydes (4R-PhC(O)H, R = CH_3O, CH_3, H, Cl, CN), and a good linear correlation was obtained with small positive Hammett ρ value of +0.48 by plotting the relative rates as a function of σ_p of the *para*-substituents. This result demonstrates that electron-donating groups on the substrate decrease and electron-withdrawing groups increase the reaction rate, and that the metal-based oxidant in that case is nucleophilic (Fig. 2D). This value is comparable to those obtained previously in the Baeyer-Villiger type deformylation of PhCHO by $[Mn^{II}Mn^{III}(O_2)(BPMP)]^{2+}$ (ρ = +0.64; HBPMP = 2,6-bis[(bis(2-pyridylmethyl)amino)methyl]-4-methylphenol),[12] and **2** (ρ = +0.67),[13b] suggesting a similar mechanism including a nucleophilic attack of the peroxide on the aldehyde C-atom in the rate-determining step (Scheme 2). These results above serve strong evidence for the ambiphilic behavior of **1**. As it is able to assist both nucleophilic and electrophilic oxidations, we have carried out competitive reactions of PhC(O)H and DTBPH, and found that nucleophilic oxidation of benzaldehyde competes with the O–O bond cleavage step required to generate the electrophilic $O=Fe^{IV}–O–Fe^{IV}=O$ (**1a**) oxidant in a preequilibrium process with steady-state kinetics ($+d[\mathbf{1a}]/dt = -d[\mathbf{1a}]/dt$; $K = k_1/k_{-1}$, where $k_1 << k_{-1}$, k_2), responsible for the phenol oxidation in the rate-determining step (k_{rds}). **1a** is formed by analogy to what Kodera has demonstrated for his diferric-peroxo intermediate by a dinucleating octadentate 6,6-(ethylene-bridged)bis(TPA) ligand.[18] The equlibrium between **1a** and **1** can also be supported based on the previously published $[Fe^{II}(IndH)(solv)_3]^{2+}$-catalyzed H_2O_2 oxidation of thioanisole and benzyl alcohol via electrophilic OAT (ρ = -0.4) and HAA (ρ = -0.85, *KIE* = 9) process, respectively.[14]

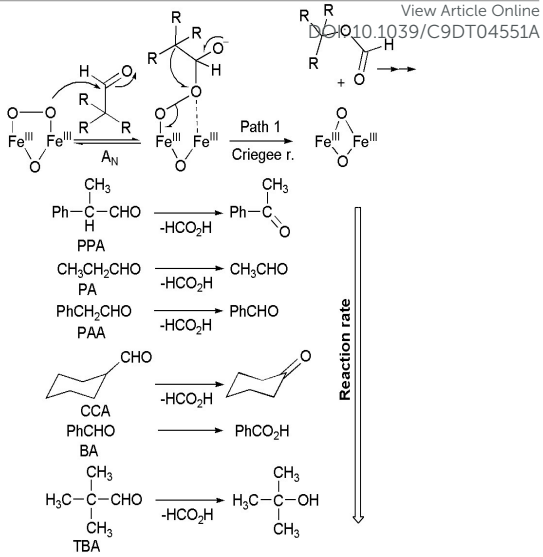

Scheme 2. Proposed mechanism for the nucleophilic reactions of **1** with series of aldehydes.

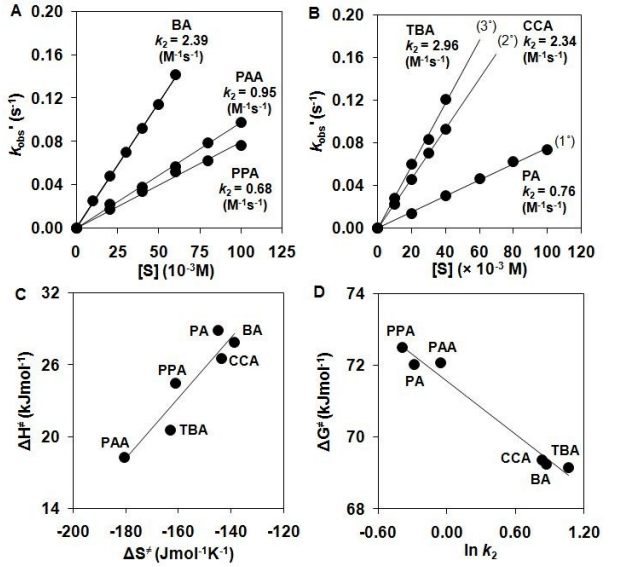

Fig. 3. Second-order rate constants (k_2) determined in the reactions of **1** (1 mM) at 10 ˚C with alkyl aryl (A) and alkyl aldehydes (B). (C) Isokinetic plot and (D) Plot of $\Delta G^{\ddagger}$ versus lnk_2 for the reaction between **1** and various aldehydes.

Finally, we have investigated the scope of substrates for the Baeyer-Villiger reaction of **1** by the use of various aryl alkyl (Fig. 3A) and alkyl aldehyde (Fig. 3B) derivatives (Scheme 2). The reactions with 2-phenylpropionaldehyde (PPA) and phenylacetaldehyde (PAA) afforded acetophenone and benzaldehyde, respectively as major reaction products based on gas chromatography mass spectrometry. The relative reactivity of **1** toward the aryl and aryl alkyl aldehydes shows the following order PhCHO > PAA > PPA (Table 1, Fig. 3A). **1** was also able to deformylates various alkyl aldehydes such as pivalaldehyde (TBA), cyclohexanecarboxaldehyde (CCA) and propionaldehyde (PA) affording *tert*-butanol, cyclohexanone and acetaldehyde, respectively as major products (Fig. S4-S8, ESI). The relative reactivity order; TBA (3˚) > CCA (2˚) > PA (1˚)

Table 1. Rate constants and activation parameters for the reaction of **1** and **2** towards aldehydes and phenols.

Substrate/ Complex	k_2[a] [$M^{-1}s^{-1}$]	ρ	$\Delta H^{\ddagger}$ [$kJmol^{-1}$]	$\Delta S^{\ddagger}$ [$Jmol^{-1}K^{-1}$]	$\Delta G^{\ddagger}$ [$kJmol^{-1}$]
TBA/**1**	2.96±0.15		21±1	-163±3	69±2
CCA/**1**	2.34±0.10		27±1	-144±5	69±3
PhCHO/**1**	2.39±0.06	+0.48	28±1	-138±3	69±2
PhCHO/**2**[13b]	0.59	+0.67	42	-98	71
PAA/**1**	0.95±0.06		18±1	-181±2	72±1
PAA/**2**[13b]	0.04		52	-87	77
PA/**1**	0.77±0.03		29±2	-145±6	72±4
PPA/**1**	0.68±0.04		25±1	-162±5	73±2
PPA/**2**[13b]	0.002		72	-34	82
DTBPH/**1**	0.40±0.01	-0.62	27±4	-175±14	79±8
DTBPH/**2**[13a]		-0.71	64	-108	96

[a]In CH_3CN at 10 ºC; $k_2 = (k_{obs} - k_{sd}) / [S]$ from $-d[\mathbf{1}]/dt = k_{obs}[\mathbf{1}] = (k_{sd} + k_2[S])[\mathbf{1}]$ (Table S1-S9, ESI).

(Fig. 3B), is typical for the Baeyer-Villiger mechanism, where the migratory ability on the Criegee intermediate is ranked tertiary (3˚) > secondary (2˚) > primary (1˚). The more electron-rich (most-substituted) alkyl group migrates in preference., which can be explained by the buildup of positive charge in the transition state for breakdown of the Criegee intermediate.[19]

These results above suggest that in the case of benzaldehydes the nucleophilic attack of the peroxide on the aldehyde C-atom, while in the case of the investigated aryl-alkyl and alkyl aldehydes the Criegee-rearrangement can be postulated as rate-determining step. Based on kinetic and activation parameters presented herein demonstrate that the *μ*-oxo-*μ*-1,2-peroxo-diferric species, **1** is much more reactive than the *μ*-1,2-peroxo-diferric species, **2** in the deformylation reactions (Table 1); e.g., the relative rate is 24 for PAA ($\Delta\Delta G^{\ddagger}$ = 5 kJ mol^{-1}), and significantly larger for PPA (k_{rel} = 340 with $\Delta\Delta G^{\ddagger}$ = 9 kJ mol^{-1}). Based on the temperature dependence of the reaction rates of the investigated formylation reactions we have also found that the values of $-T\Delta S^{\ddagger}$ in the studied temperature range, were larger than $\Delta H^{\ddagger}$, indicating an entropy-controlled reaction (Fig. 3C, Fig. S9, ESI), contrary to that observed for **2** (Table 1, enthalpy-controlled reaction with $\Delta H^{\ddagger} > T\Delta S^{\ddagger}$). Arbitrary fitting of a linear relationship to available entropy and enthalpy data yields $\Delta H^{\ddagger}$ = 63.4 kJ mol^{-1} at the intercept, which is little bit smaller than that was obtained for the deformylation reaction of **2**. Furthermore, the calculated Gibbs energy values correlate very well with the reaction rates (Fig. 3D).

Efforts have been made to find strong evidence for the ambiphilic behavior of non-heme peroxo-diferric intermediate. We have found that the μ-oxo-μ-1,2-peroxo-diferric intermediate is capable of deformylating aldehydes via nucleophilic, and able to oxidize phenols via an electrophilic reaction with significantly larger rates than those observed for the previously reported μ-1,2-peroxo-diferric species. Based on detailed kinetic studies, a plausible mechanism has been proposed for both systems, and the relative reactivity values have been discussed in details. Studies on the oxidation of hydrocarbons as further evidence for the formation of **1a** including DFT calculations are in progress.

Notes and references

Conflicts of interest: There are no conflicts of interest to declare.

§ This work was supported by a grant from The Hungarian National Research Fund (OTKA) K108489 and GINOP-2.3.2-15-2016-00049.

1 P. Nordlund, P. Reichard, *Annu. Rev. Biochem*., 2006, **75**, 681.
2 T. M. Makris, V. V. Vu, K. K. Meier, A. J. Komor, B. S. Rivard, E. Münck, L. Que, Jr., J. D. Lipscomb, *J. Am. Chem. Soc*., 2015, **137,** 1608.
3 (a) Z. Han, N. Sakai, L. H. Boettger, S. Klinke, J. Hauber, A. X. Trautwein, R. Hilgenfeld, *Structure* 2015, **23**, 882; (b) V. V. Vu, J. P. Emerson, M. Martinho, Y. S. Kim, E. Münck, M. H. Park, L. Que, Jr., *Proc. Nat. Acad. Sci. U.S.A.,* 2009, **106**, 14814; (c) M. H. Park, *J. Biochem.,* 2006, **139**, 161.
4 (a) B. J. Wallar, J. D. Lipscomb, *Chem. Rev*., 1996, **96**, 2625; (b) C. E. Tinberg, S. J. Lippard, *Acc. Chem. Res*., 2011, **44**, 280.
5 (a) A. D. Bochevarov, J. Li, W. J. Song, R. A. Friesner, S. J. Lippard, *J. Am. Chem. Soc.,* 2011, **133**, 7384; (b) L. M. Newman, L. P. Wackett, *Biochemistry* 1995, **34**, 14066; (c) J. M. Studts, K. H. Mitchell, J. D. Pikus, K. McClay, R. J. Steffan, B. G. Fox, *Protein Expr. Purif*., 2000, **20**, 58; (d) W. J. Song, R. K. Behan, S. G. Naik, B. H. Huynh, S. J. Lippard, *J. Am. Chem. Soc.,* 2009, **131**, 6074.
6 (a) A. Trehoux, J.-P. Mahy, F. Avenier, *Coord. Chem. Rev.,* 2016, **322**, 142; (b) A. J. Jasniewski, L. Que, Jr. *Chem. Rev.,* 2018, **118**, 2554.
7 (a) A. Schirmer, M. A. Rude, X. Li, E. Popova, S. B. del Cardayre, *Science* 2010, **329**, 559; (b) N. Li, W.-C. Chang, D. M. Warui, S. J. Booker, C. Krebs, J. M. Bollinger, *Biochemistry* 2012, **51**, 7908; (c) C. Krebs, J. M. Bollinger, Jr., S. J. Booker, *Curr. Opin. Chem. Biol.,* 2011, **15**, 291; (d) C. Jia, M. Li, J. Li, J. Zhang, H. Zhang, P. Cao, X. Pan, X. Lu, W. Chang, *Protein. Cell*., 2015, **6**, 55.
8 (a) T. Abe, Y. Morimoto, T. Tano, K. Mieda, H. Sugimoto, N. Fujieda, T. Ogura, S. Itoh, *Inorg. Chem.*, 2014, **53**, 8786; (b) T. Tano, Y. Okubo, A. Kunishita, M. Kubo, H. Sugimoto, N. Fujieda, T. Ogura, S. Itoh, *Inorg. Chem.*, 2013, **52**, 10431.
9 (a) S. Hong, K. D. Sutherlin, J. Park, E. Kwon, M. A. Siegler, E. I. Solomon, W. Nam, *Nat. Commun.*, 2014, **5**, 5440; (b) K. Ray, F. F. Pfaff, B. Wang, W. Nam, *J. Am. Chem. Soc.*, 2014, **136**, 13942.
10 X. Shan, L. Que, Jr., *Proc. Natl. Acad. Sci.*, 2005, **102**, 5340.
11 M. J. Park, J. Lee, Y. Suh, J. Kim, W. Nam, *J. Am. Chem. Soc.*, 2006, **128**, 2630.
12 A. M. Magherusan, S. Kal, D. N. Nelis, L. M. Doyle, E. R. Farquhar, L. Que, Jr., A. R. McDonald, *Angew. Chem. Int. Ed.* 2019, **58**, 5718.
13 (a) M. I. Szávuly, M. Surducan, E. Nagy, M. Surányi, G. Speier, R. Silaghi-Dumitrescu, J. Kaizer, *Dalton Trans.*, 2016, **45**, 14709; (b) B. Kripli, F. V. Csendes, P. Török, G. Speier, J. Kaizer, *Chemistry - A European Journal*, 2019, 25, 14290; (c) S. V. Kryatov, S. Taktak, I. V. Korendovych, E. V. Rybak-Akimova, J. Kaizer, S. Torelli, X. Shan, S. Mandal, V. L. MacMurdo, A. Mairata i Payeras, L. Que, Jr., *Inorg. Chem*., 2005, **44**, 85; (d) M. A. Cranswick, K. K. Meier, X. Shan, A. Stubna, J. Kaizer, M. P. Mehn, E. Münck, L. Que, Jr., *Inorg.*

View Article Online
DOI: 10.1039/C9DT04551A

Chem., 2012, **51**, 10417; (e) A. T. Fiedler, X. Shan, M. P. Mehn, J. Kaizer, S. Torelli, J. R. Frisch, M. Kodera, L. Que, Jr., *J. Phys. Chem. A.* 2008, **112**, 13037; (f) J. S. Pap, A. Draksharapu, M. Giorgi, W. R. Browne, J. Kaizer, G. Speier, *Chem. Commun.*, 2014, **50**, 1326.

14 J. S. Pap, M. A. Cranswick, É. Balogh-Hergovich, G. Baráth, M. Giorgi, G. T. Rohde, J. Kaizer, G. Speier, L. Que, Jr., *Eur. J. Inorg. Chem.*, 2013, 3858;

15 D. Lakk-Bogáth, G. Speier, J. Kaizer, *Polyhedron*, 2018, **145**, 227.

16 K. Nehru, Y. Jang, S. Oh, F. Dallemer, W. Nam, J. Kim, *Inorg. Chim. Acta*, 2008, **361**, 2557.

17 (a) R. A. Binstead, M. E. McGuire, A. D. Dovletoglou, W. K. Seok, L. E. Roecker, T. J. Meyer, *J. Am. Chem. Soc.*, 1992, **114**, 173; (b) C. V. Sastri, J. Lee, K. Oh, Y. J. Lee, J. Lee, T. A. Jackson, K. Ray, H. Hirao, W. Shin, J. A. Halfen, J. Kim, L. Que, Jr., S. Shaik, W. Nam, *Proc. Natl. Acad. Sci. U.S.A.*, 2007, **104**, 19181.

18 M. Kodera, M. Itoh, K. Kano, T. Funabiki, M. Reglier, *Angew. Chem. Int. Ed.*, 2005, **44**, 7104.

19 (a) G.-J. Brink, W. C. E. Arends, R. A. Sheldon, *Chem. Rev.*, 2004, **104**, 4105; (b) M. F. Hawthorne, W. D. Emmons, K. S. McCallum, *J. Am. Chem. Soc.*, 1958, **80**, 6393.

Functional models of nonheme diiron enzymes: reactivity of μ-oxo-μ-1,2-peroxo-diiron(III) intermediate in electrophilic and nucleophilic reactions.

View Article Online
DOI: 10.1039/C9DT04551A

Balázs Kripli, Miklós Szávuly, Flóra Viktória Csendes, and József Kaizer*

The ambiphilic behavior (electrophilic versus nucleophilic character) of peroxo-diferric complex, and its relative reactivity towards aldehydes and phenols has been discussed.